The Relationship Between the ITCZ and the Southern Hemispheric Eddy-Driven Jet

Paulo Ceppi,[1] Yen-Ting Hwang,[1] Xiaojuan Liu,[1] Dargan M. W. Frierson,[1]

and Dennis L. Hartmann[1]

P. Ceppi, Department of Atmospheric Sciences, University of Washington, Box 351640, Seattle, Washington 98195-1640, USA. (ceppi@atmos.washington.edu)

Y.-T. Hwang, Department of Atmospheric Sciences, University of Washington, Box 351640, Seattle, Washington 98195-1640, USA. (yting@atmos.washington.edu)

X. Liu, Department of Atmospheric Sciences, University of Washington, Box 351640, Seattle, Washington 98195-1640, USA. (xjliu@atmos.washington.edu)

D. M. W. Frierson, Department of Atmospheric Sciences, University of Washington, Box 351640, Seattle, Washington 98195-1640, USA. (dargan@atmos.washington.edu)

D. L. Hartmann, Department of Atmospheric Sciences, University of Washington, Box 351640, Seattle, Washington 98195-1640, USA. (dennis@atmos.washington.edu)

[1]Department of Atmospheric Sciences,
University of Washington, Seattle,
Washington, USA.

Abstract.

We study the effect of a thermal forcing confined to the midlatitudes of one hemisphere on the eddy-driven jet in the opposite hemisphere. We demonstrate the existence of an "interhemispheric teleconnection," whereby warming (cooling) the Northern Hemisphere causes both the intertropical convergence zone (ITCZ) and the Southern Hemispheric midlatitude jet to shift northward (southward). The interhemispheric teleconnection is effected by a change in the asymmetry of the Hadley cells: as the ITCZ shifts away from the Equator, the cross-equatorial Hadley cell intensifies, fluxing more momentum toward the subtropics and sustaining a stronger subtropical jet. Changes in subtropical jet strength, in turn, alter the propagation of extratropical waves into the tropics, affecting eddy momentum fluxes and the eddy-driven westerlies. The relevance of this mechanism is demonstrated in the context of future climate change simulations, where shifts of the ITCZ are significantly related to shifts of the Southern Hemispheric eddy-driven jet in austral winter. The possible relevance of the proposed mechanism to paleoclimates is discussed, particularly with regard to theories of ice age terminations.

1. Introduction

A fundamental question in atmospheric dynamics is to understand meridional shifts of the zonally-averaged circulation, and particularly of the zonal-mean midlatitude jet. In the context of anthropogenic climate change, the effect of global warming on the latitude of the eddy-driven jet has received much attention in the recent literature [e.g., *Hartmann et al.*, 2000; *Kushner et al.*, 2001; *Chen and Held*, 2007; *Lorenz and DeWeaver*, 2007; *Kidston et al.*, 2011]. There exist, however, a variety of mechanisms that may force shifts of the eddy-driven westerlies. The purpose of this study is to propose one such mechanism, which involves a shift of the intertropical convergence zone (ITCZ) and a change in the asymmetry of the Hadley cells.

While it is well established that the eddy-driven midlatitude jet and the tropical Hadley circulation can mutually influence each other, the mechanisms and the causal relations behind such interactions may be quite diverse. Extratropical eddies, via their fluxes of heat and momentum, have been shown to influence the Hadley circulation both in terms of strength and meridional extent [e.g., *Walker and Schneider*, 2006; *Caballero*, 2007; *Kang and Polvani*, 2011; *Ceppi and Hartmann*, in press]. However, it is known that the converse situation is also possible, where changes in the Hadley circulation cause a response of the eddy-driven jet. This happens because the Hadley circulation controls the strength of the subtropical jet through the meridional advection of momentum in the upper tropical troposphere [*Chang*, 1995; *Seager et al.*, 2003]. In turn, the subtropical jet interacts with the eddy-driven jet, due to its effects on baroclinicity [*Lee and Kim*, 2003;

Brayshaw et al., 2008] and on barotropic wave propagation [*Eichelberger and Hartmann*, 2007; *Barnes and Hartmann*, 2011].

A major influence on Hadley cell strength and ITCZ latitude is the interhemispheric thermal gradient [*Broccoli et al.*, 2006; *Kang et al.*, 2008; *Frierson and Hwang*, 2012; *Donohoe et al.*, in press]. Temperature asymmetries between the hemispheres cause a shift of the ITCZ toward the warmer hemisphere and a strengthening of the Hadley cell in the colder hemisphere, and this appears prominently in the seasonal cycle of the Hadley circulation, with the winter cell being much stronger than the summer one [*Lindzen and Hou*, 1988; *Dima and Wallace*, 2003]. It is thus possible that substantial changes in ITCZ latitude and in Hadley cell strength, particularly due to variations in the interhemispheric thermal gradient, could induce a change in subtropical jet strength and therefore a shift of the westerlies.

Recent work has suggested a possible linkage between meridional shifts of the ITCZ and of the eddy-driven westerlies in the context of ice age terminations, where the ITCZ shift may have been forced mainly from the Northern Hemisphere (NH) [*Anderson et al.*, 2009; *Toggweiler and Lea*, 2010; *Denton et al.*, 2010]. The Southern Hemispheric (SH) eddy-driven jet shift induced by the change in tropical circulation may in turn have caused a change in ocean circulation, leading to enhanced venting of CO_2 from the deep ocean. This would have warmed the climate globally, bringing the ice age to an end. In experiments with a coupled atmosphere–ocean general circulation model, *Lee et al.* [2011] demonstrated that anomalous cooling in the North Atlantic can trigger a response of the SH eddy-driven jet leading to increased venting of CO_2, although they focused on changes in jet strength instead of latitude.

The primary purpose of this study is to explore the dynamical processes involved in the remote response of the eddies to a forcing in the opposite hemisphere. Using idealized model experiments, we show that the eddy-driven jet responds to thermal forcings confined to the midlatitudes of the opposite hemisphere. We then demonstrate that the eddy response can be explained by the change in Hadley cell strength associated with a shift of the ITCZ, and show the relevance of this tropical control mechanism in the context of future climate change.

2. Data and Methods

2.1. Model experiments

Three different models are used in this study to investigate the relationship between the strength of the subtropical jet and the latitude of the eddy-driven jet.

The effect of interhemispheric thermal gradients on the zonal-mean circulation is tested in the GFDL AM2.1 model [*The GFDL Global Atmospheric Model Development Team*, 2004] in aquaplanet configuration. The lower boundary is a slab mixed-layer ocean with a depth of 50 m [*Manabe and Stouffer*, 1980], and the model is run under perpetual equinox conditions. Model output is averaged over the last six years of each simulation, after a two-year spinup. The model is run at a horizontal resolution of 2° latitude × 2.5° longitude with 24 levels. The interhemispheric thermal gradient is varied by imposing an anomalous energy flux (a "Q-flux") at the ocean surface in the midlatitudes of the Northern Hemisphere only. The anomalous Q-flux is modeled as a Gaussian function of latitude:

$$Q(\phi) = A \exp\left[-\frac{(\phi - \phi_m)^2}{2\sigma^2}\right]. \quad (1)$$

We set $\phi_m = 50°$ N, $\sigma = 7°$, and A is varied from -50 to $+50$ W m^{-2} in 10-W m^{-2} increments. Note that because there is no energy source or sink to compensate for the anomalous Q-flux in the NH midlatitudes, energy is not conserved in the perturbed runs.

To assess the applicability of our results to a more realistic atmosphere, we run similar experiments in the ECHAM atmospheric general circulation model version 4.6 [hereafter ECHAM4.6; *Roeckner et al.*, 1996], which includes real-world land distribution and topography. The atmospheric model is run in T42 resolution with 19 vertical levels, and is coupled to a slab ocean, with a 50-m mixed layer. In the control case, ocean heat transport is simulated by applying Q-fluxes, which were calculated to maintain a seasonal cycle of ocean temperatures that is as close as possible to present-day conditions. In addition to the control Q-fluxes, we carry out an experiment with a Q-flux perturbation following Eq. 1, with an amplitude $A = -100$ W m^{-2}. This is similar to the aquaplanet experiments except for the fact that the forcing is restricted to ocean gridpoints in the NH, resulting in a zonal-mean forcing amplitude of -44 W m^{-2}.

Finally, we employ a simple barotropic model to investigate the interactions between the subtropical jet and the eddies. The model setup is as in *Vallis et al.* [2004] and *Barnes and Hartmann* [2011] and we refer the reader there for details, but summarize the main points in the following. The model integrates the nondivergent barotropic vorticity equation on the sphere, with linear damping of vorticity and fourth-order diffusion. Eddies are generated by stochastic vorticity stirring, which is centered at 50° N and windowed with a Gaussian mask in meridional direction. The strength of the stirring is the same as in *Barnes and Hartmann* [2011], chosen to simulate a midlatitude storm track of realistic intensity. In addition to the stirring, a subtropical jet of varying strength is prescribed,

as in *Barnes and Hartmann* [2011]:

$$u_{\mathrm{sub}}(\phi) = U \exp\left[-\frac{(\phi - \phi_{\mathrm{sub}})^2}{2\sigma_{\mathrm{sub}}^2}\right], \tag{2}$$

where ϕ denotes latitude and u zonal wind. Hence, the subtropical jet is a Gaussian in latitude, with a width $\sigma_{\mathrm{sub}} = 6°$, a center at $\phi_{\mathrm{sub}} = 25°$, and an amplitude U ranging from 0 to 25 m s^{-1} in increments of 5 m s^{-1}. Each integration is averaged over 8000 days, after discarding 500 days of spinup.

2.2. CCSM3 21st century integrations

We make use of a 30-member ensemble of 21st-century simulations of the Community Climate System Model Version 3 (CCSM3) coupled general circulation model [*Collins et al.*, 2006]. All members are subject to the same external forcing, following the A1B greenhouse gas emission scenario [*Houghton et al.*, 2001]. This large ensemble of integrations has been described in detail in *Deser et al.* [2010], *Branstator and Teng* [2010], and *Meehl et al.* [2010], and we mention only the important points here. The initial conditions are taken from a single 20th-century integration of CCSM3. The atmospheric component of the model is started from different initial conditions in each simulation, corresponding to different days in December 1999 or January 2000. The ocean, ice, and land components, however, are all branched from 1 January 2000 and thus have identical initial conditions. All integrations are run for 62 years, from January 2000 to December 2062.

We estimate changes in eddy-driven jet latitude and tropical circulation asymmetry (see definitions below) by averaging model output over the last 20 years of each integration (i.e., 2043–2062). Because all ensemble members are started from the same 20th-century

integration, the different climatologies in 2043–2062 reflect different evolutions of the eddy-driven jet and of the tropical circulation asymmetry.

2.3. CMIP5 data

In addition to our model experiments, we also investigate the relationship between SH jet latitude and the asymmetry of the Hadley cells in Coupled Model Intercomparison Project phase 5 (CMIP5) model simulations based on the RCP8.5 emission scenario [*Taylor et al.*, 2012]. The variables used are monthly-mean zonal and meridional wind, air temperature, and precipitation, covering the time period 2000–2099. (Since RCP8.5 integrations start in 2006, the last six years of the historical integrations were used to obtain a 100-year dataset for each model.) Table 1 lists the 35 models used in this study, of which only the first ensemble member was considered. The values were aggregated in seasonal and annual resolution to calculate linear trends, using least-squares regression.

2.4. ITCZ latitude and tropical circulation asymmetry

We quantify the ITCZ latitude and the associated tropical circulation asymmetry using two indices. We define a tropical precipitation asymmetry index, $\Delta P = 100 \times (P_{\mathrm{NH}} - P_{\mathrm{SH}})/(P_{\mathrm{NH}} + P_{\mathrm{SH}})$, where P_{NH} and P_{SH} represent the total precipitation falling within 20° of the Equator in the NH and SH, respectively. We also use a cross-equatorial mass flux index Ψ_0, defined as the value of the meridional mass streamfunction (see definition below) at 500 hPa at the Equator. By definition, both ΔP and Ψ_0 are positive when the ITCZ is north of the Equator.

2.5. Eddy-driven jet latitude, Hadley cell strength indices, and eddy fluxes

Throughout the paper, we define the location of the midlatitude (or eddy-driven) jet as the latitude of the maximum zonally-averaged zonal wind at the surface, or at 850 hPa in ECHAM and CMIP5 model output, to avoid complications with grid boxes below surface level. The zonal wind distribution is cubically interpolated in latitude (using the four nearest neighbor gridpoints) at a resolution of 0.1° prior to determining the eddy-driven jet latitude. The meridional mass streamfunction is calculated as the vertically-integrated, mass-weighted meridional wind $\bar{v}$, $\Psi = 2\pi a g^{-1} \int_0^p \bar{v} \cos\phi \, dp'$, where a represents the radius of the Earth and other symbols have their usual meaning. The strength of the Hadley cell is then simply the maximum absolute value of Ψ within the cell. Finally, we calculate eddy momentum fluxes using daily zonal and meridional wind anomalies. Because we perform model experiments with no seasonal cycle, the anomalies are simply defined as departures from the zonally-averaged, time-mean winds.

3. Results

3.1. Latitude of the ITCZ and of the eddy-driven jet in an aquaplanet model

Changes in interhemispheric thermal gradients are known to influence the latitude of the ITCZ by inducing a shift toward the warmer hemisphere [e.g., *Broccoli et al.*, 2006; *Kang et al.*, 2008]. Similar behavior is observed in our aquaplanet model experiments (Fig. 1): the boundary between the two Hadley cells shifts by about 20 degrees between the experiments with $A = \pm 50$ W m^{-2}. Associated with the ITCZ shift is an asymmetry in Hadley cell strength, with the cross-equatorial Hadley cell being much stronger [*Dima and Wallace*, 2003].

As A increases and the ITCZ shifts northward, the strengthening of the SH Hadley cell induces an increase in zonal momentum advection by the mean circulation. This corresponds to an intensification of the upper-tropospheric subtropical jet, which is sustained by the convergence of westerly momentum by the Hadley and Ferrel cells. The maximum in convergence of momentum flux in the subtropics (near 30° S) is well visible in the top panel of Fig. 2. Hence, in a zonal-mean framework, shifts of the ITCZ are associated with changes in subtropical jet strength.

Perhaps more surprising is the fact that the SH eddy-driven jet (vertical black lines in Fig. 1) also responds to the thermal forcing in the NH, such that it shifts equatorward as the SH Hadley cell and subtropical jet strengthen. This is consistent with the change in eddy momentum flux convergence shown in the bottom panel of Fig. 2. Because the anomalous heating is restricted to the midlatitudes of the NH, the remote forcing of the SH jet must be effected by a change in the tropical circulation. We plot a wider range of experiments with varying A as a function of ITCZ latitude and SH Hadley cell strength in Fig. 3. While the Hadley cell strength is nearly linearly related to the latitude of the ITCZ, the relationship between eddy-driven jet latitude and Hadley cell strength is somewhat more complex. When the Hadley cell (or the subtropical jet) is very strong, the SH eddy-driven jet is located at a relatively low latitude, near 42° S, and is merged with the subtropical jet in the upper troposphere (cf. bottom panel of Fig. 1). In this regime the eddy-driven jet does not shift much for varying Hadley cell strengths, as it is bounded by the subtropical jet on its equatorward flank. For Hadley cells weaker than about 250 Sv, however, the response of the eddy-driven jet to changes in Hadley cell strength is larger.

It is important to note that the eddy-driven jet response cannot be explained by the global warming or cooling induced by the NH Q-flux forcings. In the cooling cases, for example, there is marked cooling in both hemispheres (Fig. 4); from this one would expect an equatorward contraction of the circulation [e.g., *Lu et al.*, 2010]. However, our results indicate that the *stronger* NH cooling, and the associated Hadley cell weakening in the SH, are more important in explaining the response of the SH jet. Hence, the change in Hadley cell and subtropical jet strength may exert a stronger influence on the eddy-driven jet latitude than the change in mean hemispheric temperature.

It is worth pointing out that the response in the hemisphere opposite to the forcing, and thus the strength of the interhemispheric teleconnection, is likely to be influenced by model-dependent cloud feedbacks. The importance of cloud effects may be inferred from the SH temperature response in Fig. 4: although there is an enhanced energy transport into the SH by the anomalous Hadley circulation when the NH is warmed, we observe slight cooling in the SH. This very likely results from changes in cloud radiative effects, which are large enough to cancel the enhanced energy transport from the NH by the Hadley circulation. While we have not investigated the details of this mechanism, this result suggests that uncertainties in cloud feedbacks may limit the ability of climate models to accurately represent the strength of the interhemispheric teleconnection.

An additional caveat is that the aquaplanet model used in this study has very strong Hadley cells in its control configuration, more akin to the wintertime than to the annual-mean Hadley cells in the real atmosphere. This is a common feature of aquaplanets in the absence of poleward ocean heat transport [*Frierson et al.*, 2006] and may explain, at least in part, the low eddy-driven jet latitude in the control simulation (right panel of Fig. 3).

It is likely that our results do not apply to summer conditions, where the Hadley cell is very weak and largely eddy-driven [*Dima and Wallace*, 2003; *Ceppi and Hartmann*, in press]. We will demonstrate later that in more realistic simulations with a seasonal cycle, a relationship between the eddy-driven jet and the ITCZ is found only in winter.

3.2. Interactions between subtropical and eddy-driven jets

We now consider the specific mechanism behind the response of the eddy-driven jet to the change in subtropical jet strength. Subtropical jets are known to interact with eddy-driven jets both from the perspective of baroclinic and barotropic processes. In terms of baroclinicity, the subtropical jet coincides with a region of strong vertical wind shear, since it is usually not associated with westerlies at the surface. Subtropical jet strengthening is thus consistent with larger vertical wind shears, and therefore increasing baroclinicity and Eady growth rates near the subtropics [see e.g. *Lee and Kim*, 2003; *Brayshaw et al.*, 2008]). In model experiments initialized with an axially symmetric state and with subtropical jets of varying strengths, *Lee and Kim* [2003] showed that the growth of the most unstable baroclinic waves tends to occur along the subtropical jet when the latter is sufficiently strong, while waves grow preferentially in midlatitudes for relatively weak subtropical jets.

From a barotropic perspective, the subtropical jet may influence the eddy-driven jet by affecting the meridional propagation of extratropical waves in the upper troposphere. A strong subtropical jet can act as a waveguide within which Rossby waves tend to remain trapped, thereby reducing the feedback of the eddies on meridional shifts of the jet [*Eichelberger and Hartmann*, 2007; *Barnes and Hartmann*, 2011; *Barnes and Polvani*, in press]. Using barotropic model experiments with a prescribed subtropical jet and

stochastic eddy stirring at different latitudes, *Barnes and Hartmann* [2011] also showed that when the subtropical jet is strong, an eddy-driven jet tends to develop on its poleward flank even as the stirring latitude increases. This is because the subtropical jet sets the latitude of wave breaking for equatorward-propagating waves when it is sufficiently strong, thereby forcing the waves to propagate to its equatorward flank and inducing convergence of momentum by the eddies on its poleward flank. Thus, there appears to be a barotropic equivalent to the baroclinic mechanism proposed by *Lee and Kim* [2003].

Here, we investigate whether the response of the eddy-driven jet to changes in subtropical jet strength observed in the aquaplanet model experiments can be explained using barotropic wave propagation arguments. To this end, we perform experiments in a barotropic model, in the same configuration as in *Barnes and Hartmann* [2011] (see Data and Methods). To quantify the influence of the subtropical jet, we stir eddies at a constant latitude of 50°, while varying the strength of a prescribed subtropical jet centered at 25°. The resulting zonal wind profiles are shown in Fig. 5 for three experiments. As the subtropical jet strengthens, the maximum eddy-driven zonal wind clearly shifts equatorward, toward the poleward flank of the subtropical jet; this happens despite the stirring latitude remaining fixed. When the subtropical jet is strongest (bottom panel of Fig. 5), the two jets are nearly merged. The eddy-driven zonal wind profile also becomes skewed toward the Equator when the subtropical jet is strong, which is due to the preferential deposition of momentum on the poleward flank of the subtropical jet (red lines in Fig. 5); this is similar to the changes observed in the aquaplanet experiments (bottom panel of Fig. 2). The effect of the subtropical jet on the eddy-driven jet latitude is summarized in Fig. 6 for a wide range of subtropical jet strengths.

To understand our results, it is helpful to consider the phase speed dependence of eddy momentum fluxes. We calculated the power spectrum of eddy momentum flux convergence $-\mathrm{div}\,\overline{u'v'}$ as a function of phase speed and latitude, following *Randel and Held* [1991]. The results are shown in Fig. 7, with $-\mathrm{div}\,\overline{u'v'}$ multiplied by the cosine of latitude to represent the torque exerted by the eddies on the mean flow. In a state with a weak subtropical jet, the latitudes of eddy momentum flux divergence and convergence are strongly dependent on the phase speed of the waves, with faster waves located at higher latitudes. As the subtropical jet strength increases, however, the "tilt" of the distribution of convergence and divergence disappears (bottom panel of Fig. 7). This results mostly from a displacement of the momentum fluxes by faster eddies toward lower latitudes, while the slower waves are relatively unaffected. An interpretation of this result is that when a strong subtropical jet is present, waves tend to propagate deeper into the subtropics, and this effect is strongest for fast waves that would otherwise reach their critical latitudes sooner. Because there is large meridional wind shear on the equatorward side of a strong subtropical jet, the critical latitudes are only weakly dependent on the phase speed of the waves, so that all waves tend to break at similar latitudes.

To confirm that the same mechanism is present in our aquaplanet model experiments, we perform the same analysis on upper-tropospheric eddy momentum fluxes in the two extreme cases of our set of experiments ($A = \pm 50$ W m^{-2}). In the weak subtropical jet case (top panel of Fig. 8), the latitudes of eddy momentum flux convergence appear to depend on the phase speed, and as a result the convergence is spread over a wide region in the midlatitudes. By contrast, in presence of a strong subtropical jet (bottom panel of Fig. 8) all of the convergence of eddy momentum flux occurs in a narrow latitude band,

close to the subtropical jet core, and there is no visible phase speed dependence in the distribution of momentum convergence. Thus, the simple wave propagation mechanism described in our barotropic model experiments appears to apply well to a more realistic atmosphere.

3.3. ECHAM model experiments

We now examine the relevance of the proposed connection between the ITCZ and the eddy-driven jet in a more realistic context. To this end, we use the ECHAM4.6 general circulation model (see Data and Methods) and perform an experiment with cooling in all ocean gridpoints in the midlatitudes of the NH. We expect such a forcing to induce a southward shift of the ITCZ and of the surface westerlies in the SH. Because the Hadley cells and the ITCZ change substantially during the seasonal cycle, we consider different seasons separately. Here we focus on the response of the SH surface winds; the response of the zonal-mean tropical precipitation, while not shown, features a distinctive southward shift in all seasons, indicative of an ITCZ displacement.

In austral winter (JJA), the response of the eddy-driven surface winds is consistent with expectations and exhibits a high degree of zonal symmetry (Fig. 9). In response to the cooling in the NH, there is a weakening of the climatological easterlies in the subtropics, especially in the ocean basins; because of the Coriolis torque on the meridional wind, this is consistent with a weaker Hadley cell. The response of the surface westerlies is dipole-like, with a weakening equatorward of about 50° S, while some strengthening is found poleward of that latitude. It is interesting to note that the amplitude of the response is strongest in the Western Pacific, where the climatological wintertime westerlies are weakest. The structure of the surface zonal wind response looks similar in the zonal mean (Fig. 10),

and the net effect is a poleward shift of the latitude of peak zonal wind from 45° to 48° S. The change in skewness of the distribution of the surface zonal wind is reminiscent of the results from the barotropic model, where the surface westerlies tend to be more skewed toward the subtropics when the subtropical jet is strong (cf. Fig. 5).

It is worth emphasizing that the austral winter response of the eddy-driven winds looks remarkably zonally symmetric, despite the zonally asymmetric character of the NH forcing. We obtained similar results by applying a 200 W m^{-2} cooling in the North Atlantic only (not shown). Because the forcing is in the extratropics, it is likely that the signal can become significantly spread out in longitude by the prevailing westerlies before affecting the Hadley circulation, even if the forcing is relatively localized. In general, however, we believe that any localized changes in subtropical jet strength would be important in explaining local changes in the structure of the SH westerlies, as would likely occur in response to localized changes in tropical heating.

The response of the SH surface winds is much smaller in other seasons than austral winter. A small shift of about one degree is found in austral spring (SON), while no measurable response is observed in the remaining seasons (not shown). The seasonality of the response can be explained by the seasonal cycle of the Hadley cell strength and of the ITCZ latitude. In austral summer, for instance, the SH Hadley cell is very weak and its strength remains unaffected by the NH forcing (67 Sv in both experiments), while the strength of the NH Hadley cell changes dramatically (283 Sv in the control, 334 Sv in the perturbed case). At the same time, the ITCZ is far south of the Equator, so that the NH Hadley cell crosses the Equator. Therefore, it appears that the anomalous Hadley

circulation induced by the thermal forcing in the NH affects primarily the strength of the cross-equatorial Hadley cell.

Recently, *Lee et al.* [2011] studied the response of the SH westerlies to anomalous cooling in the North Atlantic that may have occurred during the last glacial termination. They found a strengthening of the surface westerlies and an enhanced wind stress on the ocean surface, which in their simulations was sufficiently strong to trigger a rise in atmospheric CO_2 between 20 and 60 ppm due to enhanced upwelling and deep ocean ventilation. Such a change in atmospheric CO_2 would have warmed the troposphere globally, likely bringing the ice age to an end. While they discussed changes in eddy-driven jet *strength* only, their results also exhibit a clear poleward shift of the SH westerlies (their Fig. 2a), particularly in JJA, consistent with our results. Unlike *Lee et al.* [2011], however, we find no significant change in the strength of the westerlies (Fig. 10). This result is not sensitive to the distribution of the forcing in the NH; we obtained very similar results with a forcing confined to the North Atlantic basin (not shown). However, it should be noted that *Lee et al.* [2011] employ a coupled atmosphere-ocean model, allowing for changes in ocean heat transport which are not possible in our simulations.

3.4. Greenhouse gas–forced shifts of the ITCZ and of the Southern Hemispheric jet

We have shown that shifts of the ITCZ may be associated with shifts of the eddy-driven jet through the control exerted by the subtropical jet on meridional wave propagation. While the current global warming trend is projected to cause a detectable poleward shift of the westerlies, particularly in the SH [*Kushner et al.*, 2001; *Kidston and Gerber*, 2010; *Barnes and Polvani*, in press], it may also induce a change in the interhemispheric thermal

gradient, due to faster warming in the NH [*Friedman et al.*, in press]. Consistent with this trend, most 21st-century climate simulations predict a northward shift of the ITCZ, as we will show in this section. Given the relationship between ITCZ shifts and changes in Hadley cell asymmetry, the rate of shifting of the ITCZ may be coupled with the rate of poleward shifting of the eddy-driven jet.

To test this hypothesis, we consider two independent sets of global warming simulations. First, we use a 30-member ensemble of integrations of the CCSM3 model, initialized from a 20th-century run (see Data and Methods). Although all ensemble members are subject to the same time-dependent external forcing (following the A1B scenario), the resulting shifts of the ITCZ and of the SH eddy-driven jet are variable among the simulations, due to differences in internal, unforced variability. We then apply a similar analysis to CMIP5 RCP8.5 integrations for the 21st century.

3.4.1. CCSM3 simulations

Because all 30 CCSM3 simulations branch off from the same late 20th-century climatology, the response of the ITCZ and of the eddy-driven jet can be assessed by averaging these quantities over the last 20 years of each integration (2043–2062), and subtracting the mean of the last 20 years of the reference 20th-century integration (1980–1999). As proxies for the latitude of the ITCZ, we use a tropical precipitation asymmetry index, ΔP, and the upper-tropospheric cross-equatorial mass flux Ψ_0 (see Data and Methods for details). These two indices are remarkably highly correlated on annual and seasonal scales ($r > 0.85$; not shown), lending confidence in the idea that they quantify the changes in ITCZ latitude and Hadley cell asymmetry in a consistent way.

The results in Fig. 11 show that changes in SH jet latitude are positively correlated with changes in ITCZ latitude among the 30 CCSM3 ensemble members. Because ΔP is defined as positive when more precipitation falls in the NH, the positive correlation implies that simulations in which the ITCZ shifts southward tend to feature a stronger poleward shift of the jet. The relationship is stronger in JJA ($r = 0.57$) than in the annual mean ($r = 0.44$), but statistically significant in both cases. Interestingly, the ensemble mean shows a southward shift of the ITCZ both in JJA and in the annual mean, contrary to the predictions of most CMIP5 models in the RCP8.5 experiments (see next section); we have not explored the causes for this behavior.

Note that in the annual mean, the distribution of points does not go through the origin, implying that part of the jet shift is unrelated to the variability in ITCZ latitude. This is likely the result of the greenhouse gas forcing, which by inducing global warming also causes a poleward shift of the jet, regardless of the change in ITCZ latitude. However, the sign of the relationship is consistent with the mechanism proposed in this paper: a northward ITCZ shift corresponds to a strengthening of the SH Hadley cell and of the subtropical jet, leading to a reduced poleward shift (or even to an equatorward shift in some ensemble members in JJA) of the SH eddy-driven jet. We verified that the change in ΔP is significantly correlated with the change in SH Hadley cell strength in the annual mean ($r = 0.61$) and in JJA ($r = 0.52$; both not shown).

One possible explanation for our results is that both the ITCZ and the SH jet are responding to variations in mean SH temperature. As discussed above, the ITCZ tends to shift toward the warmer hemisphere, while the eddy-driven jet tends to be at higher latitudes when the troposphere warms. In the hypothetical case that the SH warms while

NH temperatures remain constant, both the jet and the ITCZ would be expected to shift southward, in which case changes in ITCZ and SH jet latitude would be correlated without any direct causal relation between the two. To test this, we calculated correlations between mean SH temperatures and eddy-driven jet latitudes, and found them to be correlated in the annual mean ($r = 0.44$), but not in JJA ($r = 0.00$; both not shown). Thus, the absence of any relationship with the mean temperature makes it plausible that the differences in ITCZ shift across ensemble members are related to the differences in SH jet shift in JJA.

Considering the full seasonal cycle (Fig. 12), it appears that the ITCZ latitude and the SH jet latitude are significantly correlated only in JJA and (marginally) in the annual mean. As discussed in section 3.1, the seasonal dependence of the relationship is expected from the fact that the subtropical jet reaches its peak strength in austral winter and is therefore more likely to exert a control on the eddy-driven jet in that season. Comparing the correlations based on ΔP and Ψ_0, we find very similar values, suggesting that the analysis is robust with respect to the ITCZ metric chosen.

We also calculated correlations between ITCZ shifts and changes in NH jet latitude, but found no significant relationships in any season. It is likely that the higher degree of zonal asymmetry in the NH obscures any relationship between the Hadley cell and the eddy-driven jet.

3.4.2. CMIP5 simulations

We performed a similar analysis on CMIP5 RCP8.5 simulations, and calculated linear trends in ITCZ indices and SH eddy-driven jet latitude for the 21st century. The results are quite similar to those obtained with the CCSM3 ensemble of simulations (Fig. 13), with a weak positive correlation ($r = 0.38$) between the trends in ΔP and jet latitude

ϕ_{jet}, indicating that the models with a stronger northward ITCZ shift also tend to have a slower rate of poleward shifting of the jet. The correlation is again higher in JJA ($r = 0.57$; right panel of Fig. 13), where 18 out of 35 models feature no significant poleward shift of the jet. Hence, about a third ($r^2 = 0.33$) of the intermodel variance in SH jet latitude trends can be related to differences in ITCZ latitude trends in austral winter. Note that similar results are obtained if the trends are normalized by global- or hemispheric-mean temperature trends (not shown), excluding the possibility that the correlations are caused by differences in the rate of global warming among models.

It is also worth pointing out that although the models show a mean northward ITCZ shift in Fig. 13, there is a mean southward shift of the SH jet, contrary to the expected relationship between ITCZ shift, Hadley cell strength, and jet latitude. This is likely explained by the competing effects of interhemispheric temperature asymmetries and global warming, with the latter effect likely dominating in the multi-model mean jet shift in Fig. 13.

Again considering the full seasonal cycle of the correlations between trends in jet latitude and trends in tropical circulation asymmetry (Fig. 14), it is evident that the relationship is clearly significant only in JJA, and marginally significant in the annual mean. Thus, the subtropical jet is likely too weak in seasons other than austral winter to exert any measurable influence on the rate of shifting of the eddy-driven jet. The seasonality of this relationship is in agreement with the results of *Lee et al.* [2011] and with our experiments with the ECHAM model. The stronger response in austral winter is consistent with a tropical control mechanism on the SH eddy-driven jet. If the jet response were controlled directly from the SH extratropics, with the SH Hadley cell and the ITCZ merely respond-

ing to an extratropical forcing, then a stronger connection might be expected in austral summer, where the Hadley cell is weak and largely eddy-driven [*Kang and Polvani*, 2011; *Ceppi and Hartmann*, in press].

As for the NH, we again found no significant relationship between the shifts of the eddy-driven jet and of the ITCZ, even in boreal winter. Additional model experiments are required to understand the response of the NH westerlies to changes in Hadley cell strength that are forced from the tropics or from the opposite hemisphere. It is worth noting that the response to ENSO has been shown to involve a strengthening of the Hadley cells and an equatorward shift of the eddy-driven jets in both hemispheres, by virtue of the mechanism described in this work [*Seager et al.*, 2003; *Lu et al.*, 2008].

4. Conclusions

We demonstrate a relationship between the latitude of the intertropical convergence zone (ITCZ) and of the eddy-driven jet, which is mediated by changes in Hadley cell intensity and subtropical jet strength. As the ITCZ shifts away from the Equator, the cross-equatorial Hadley cell intensifies markedly, inducing a strengthening of the associated subtropical jet. The eddy-driven jet responds by shifting toward lower latitudes, nearer the subtropical jet. The eddy response can be explained by the effect of the subtropical jet on equatorward-propagating extratropical waves. When the subtropical jet strengthens, Rossby waves propagate deeper into the tropics, inducing enhanced convergence of eddy momentum flux on the poleward flank of the subtropical jet. The relationship between the ITCZ and the extratropical jet is such that both tend to shift in the same direction.

Due to the strong seasonal cycle of the Hadley cell, the linkage between the ITCZ and the eddy-driven jet is present mainly in the winter season, and to a lesser extent in the

annual mean. In many 21st-century global warming simulations, the ITCZ is predicted to shift because of different warming rates in the two hemispheres. We find that the ITCZ displacements are significantly correlated with Southern Hemispheric jet shifts in CMIP5 RCP8.5 model integrations in austral winter (JJA) and in the annual mean, while no significant relationships are found in the Northern Hemisphere. In the Southern Hemisphere, about a third of the intermodel variability in the jet latitude trends appears to be related to variations in ITCZ shifts in JJA. The stronger response in austral winter reflects the higher sensitivity of the Southern eddy-driven westerlies to tropical control when the Hadley cell and the subtropical jet are strong.

By virtue of the relationship proposed in this work, the eddy-driven jet can respond to thermal forcings confined to the opposite hemisphere. This highlights the existence of a dynamical "interhemispheric teleconnection" between the extratropics of both hemispheres. Apart from its relevance to future climate change, a promising application of our results is in the context of paleoclimate. Over long time scales, changes in orbital parameters and ocean circulations may have induced substantial changes in the interhemispheric temperature difference [*Chiang*, 2009; *Toggweiler and Lea*, 2010], and it is possible that joint shifts of the ITCZ and of the westerlies have taken place. Recent studies have suggested that such shifts, with their effect on ocean circulations and venting of CO_2 from the deep ocean, may have played a key role in ice age terminations [*Anderson et al.*, 2009; *Toggweiler*, 2009; *Denton et al.*, 2010; *Lee et al.*, 2011]. Additional work is needed to investigate the possible significance of the link between ITCZ and extratropical westerlies in paleoclimates.

Finally, the representation of this interhemispheric teleconnection in climate models is likely to depend on cloud feedbacks. While we have not assessed the importance of cloud effects in our model simulations, cloud feedbacks have been shown to play a crucial role in determining the ITCZ response to extratropical forcings [*Kang et al.*, 2008; *Frierson and Hwang*, 2012], and they may also modulate the propagation of the thermal forcing from the tropics to the opposite hemisphere. This highlights the importance of an accurate representation of clouds in climate models in order to improve our understanding of tropical–extratropical interactions.

Acknowledgments. We gratefully acknowledge Sarah Kang, Isaac Held, and one anonymous reviewer for their constructive comments which helped improve the paper. In addition, we thank Elizabeth Barnes for providing the barotropic model code, Qinghua Ding for modeling assistance and for setting up the slab ocean component of the ECHAM model, and Mike Wallace for helpful discussions. We thank the CCSM Climate Variability and Climate Change Working Groups "21st Century CCSM3 Large Ensemble Project" for providing their model output. We also acknowledge the World Climate Research Programme's Working Group on Coupled Modelling, which is responsible for CMIP, and we thank the climate modeling groups (listed in Table 1 of this paper) for producing and making available their model output. For CMIP the U.S. Department of Energy's Program for Climate Model Diagnosis and Intercomparison provides coordinating support and led development of software infrastructure in partnership with the Global Organization for Earth System Science Portals. This work was supported by the National Science Foundation. PC and DLH were funded by grant AGS-0960497, YTH and DMWF by grants AGS-0846641 and AGS-0936059, and XL by grants EAR-0908558 and EAR-1210920.

References

Anderson, R. F., S. Ali, L. I. Bradtmiller, S. H. H. Nielsen, M. Q. Fleisher, B. E. Anderson, and L. H. Burckle, Wind-driven upwelling in the Southern Ocean and the deglacial rise in atmospheric CO_2, *Science (New York, N.Y.)*, *323*, 1443–8, 2009.

Barnes, E. A., and D. L. Hartmann, Rossby Wave Scales, Propagation, and the Variability of Eddy-Driven Jets, *Journal of the Atmospheric Sciences*, *68*, 2893–2908, 2011.

Barnes, E. A., and L. M. Polvani, Response of the midlatitude jets and of their variability to increased greenhouse gases in the CMIP5 models, *Journal of Climate*, in press.

Branstator, G., and H. Teng, Two Limits of Initial-Value Decadal Predictability in a CGCM, *Journal of Climate*, *23*, 6292–6311, 2010.

Brayshaw, D. J., B. Hoskins, and M. Blackburn, The Storm-Track Response to Idealized SST Perturbations in an Aquaplanet GCM, *Journal of the Atmospheric Sciences*, *65*, 2842–2860, 2008.

Broccoli, A. J., K. A. Dahl, and R. J. Stouffer, Response of the ITCZ to Northern Hemisphere cooling, *Geophysical Research Letters*, *33*, L01,702, 2006.

Caballero, R., Role of eddies in the interannual variability of Hadley cell strength, *Geophysical Research Letters*, *34*, L22,705, 2007.

Ceppi, P., and D. L. Hartmann, On the Speed of the Eddy-Driven Jet and the Width of the Hadley Cell, *Journal of Climate*, in press.

Chang, E. K. M., The Influence of Hadley Circulation Intensity Changes on Extratropical Climate in an Idealized Model, *Journal of the Atmospheric Sciences*, *52*, 2006–2024, 1995.

Chen, G., and I. M. Held, Phase speed spectra and the recent poleward shift of Southern Hemisphere surface westerlies, *Geophysical Research Letters*, *34*, L21,805, 2007.

Chiang, J. C., The Tropics in Paleoclimate, *Annual Review of Earth and Planetary Sciences*, *37*, 263–297, 2009.

Collins, W. D., et al., The Community Climate System Model Version 3 (CCSM3), *Journal of Climate*, *19*, 2122–2143, 2006.

Denton, G. H., R. F. Anderson, J. R. Toggweiler, R. L. Edwards, J. M. Schaefer, and A. E. Putnam, The last glacial termination, *Science (New York, N.Y.)*, *328*, 1652–6, 2010.

Deser, C., A. Phillips, V. Bourdette, and H. Teng, Uncertainty in climate change projections: the role of internal variability, *Climate Dynamics*, *38*, 527–546, 2010.

Dima, I. M., and J. M. Wallace, On the Seasonality of the Hadley Cell, *Journal of the Atmospheric Sciences*, *60*, 1522–1527, 2003.

Donohoe, A., J. Marshall, D. Ferreira, and D. McGee, The relationship between ITCZ location and cross equatorial atmospheric heat transport; from the seasonal cycle to the last glacial maximum, *Journal of Climate*, in press.

Eichelberger, S. J., and D. L. Hartmann, Zonal Jet Structure and the Leading Mode of Variability, *Journal of Climate*, *20*, 5149–5163, 2007.

Friedman, A. R., Y.-T. Hwang, J. C. H. Chiang, and D. M. W. Frierson, Interhemispheric Temperature Asymmetry over the 20th Century and in Future Projections, *Journal of Climate*, in press.

Frierson, D. M. W., I. M. Held, and P. Zurita-Gotor, A Gray-Radiation Aquaplanet Moist GCM. Part I: Static Stability and Eddy Scale, *Journal of the Atmospheric Sciences*,

544 *63*, 2548–2566, 2006.

545 Frierson, D. M. W., and Y.-T. Hwang, Extratropical Influence on ITCZ Shifts in Slab
546 Ocean Simulations of Global Warming, *Journal of Climate*, *25*, 720–733, 2012.

547 Hartmann, D. L., J. M. Wallace, V. Limpasuvan, D. W. J. Thompson, and J. R. Holton,
548 Can ozone depletion and global warming interact to produce rapid climate change?,
549 *Proceedings of the National Academy of Sciences*, *97*, 1412–1417, 2000.

550 Houghton, J. T., Y. Ding, D. J. Griggs, M. Noguer, D. Xiaosu, and P. J. van der Linden
551 (Eds.), *Climate Change 2001: The Scientific Basis*, Cambridge University Press, 2001.

552 Kang, S. M., I. M. Held, D. M. W. Frierson, and M. Zhao, The Response of the ITCZ
553 to Extratropical Thermal Forcing: Idealized Slab-Ocean Experiments with a GCM,
554 *Journal of Climate*, *21*, 3521–3532, 2008.

555 Kang, S. M., and L. M. Polvani, The Interannual Relationship between the Latitude of
556 the Eddy-Driven Jet and the Edge of the Hadley Cell, *Journal of Climate*, *24*, 563–568,
557 2011.

558 Kidston, J., and E. P. Gerber, Intermodel variability of the poleward shift of the austral
559 jet stream in the CMIP3 integrations linked to biases in 20th century climatology,
560 *Geophysical Research Letters*, *37*, L09,708, 2010.

561 Kidston, J., G. K. Vallis, S. M. Dean, and J. A. Renwick, Can the Increase in the Eddy
562 Length Scale under Global Warming Cause the Poleward Shift of the Jet Streams?,
563 *Journal of Climate*, *24*, 3764–3780, 2011.

564 Kushner, P. J., I. M. Held, and T. L. Delworth, Southern Hemisphere Atmospheric Cir-
565 culation Response to Global Warming, *Journal of Climate*, *14*, 2238–2249, 2001.

Lee, S., and H.-K. Kim, The Dynamical Relationship between Subtropical and Eddy-Driven Jets, *Journal of the Atmospheric Sciences*, *60*, 1490–1503, 2003.

Lee, S.-Y., J. C. H. Chiang, K. Matsumoto, and K. S. Tokos, Southern Ocean wind response to North Atlantic cooling and the rise in atmospheric CO_2 : Modeling perspective and paleoceanographic implications, *Paleoceanography*, *26*, PA1214, 2011.

Lindzen, R. S., and A. V. Hou, Hadley Circulations for Zonally Averaged Heating Centered off the Equator, *Journal of the Atmospheric Sciences*, *45*, 2416–2427, 1988.

Lorenz, D. J., and E. T. DeWeaver, Tropopause height and zonal wind response to global warming in the IPCC scenario integrations, *Journal of Geophysical Research*, *112*, D10,119, 2007.

Lu, J., G. Chen, and D. M. W. Frierson, Response of the Zonal Mean Atmospheric Circulation to El Niño versus Global Warming, *Journal of Climate*, *21*, 5835–5851, 2008.

Lu, J., G. Chen, and D. M. W. Frierson, The Position of the Midlatitude Storm Track and Eddy-Driven Westerlies in Aquaplanet AGCMs, *Journal of the Atmospheric Sciences*, *67*, 3984–4000, 2010.

Manabe, S., and R. J. Stouffer, Sensitivity of a global climate model to an increase of CO_2 concentration in the atmosphere, *Journal of Geophysical Research*, *85*, 5529, 1980.

Meehl, G. A., A. Hu, and C. Tebaldi, Decadal Prediction in the Pacific Region, *Journal of Climate*, 2010.

Randel, W. J., and I. M. Held, Phase Speed Spectra of Transient Eddy Fluxes and Critical Layer Absorption, *Journal of the Atmospheric Sciences*, *48*, 688–697, 1991.

588 Roeckner, E., et al., The atmospheric general circulation model ECHAM4: Model de-
589 scription and simulation of present-day climate, *Tech. rep.*, Max Planck Institute for
590 Meteorology, 1996.

591 Seager, R., N. Harnik, Y. Kushnir, W. Robinson, and J. Miller, Mechanisms of Hemi-
592 spherically Symmetric Climate Variability, *Journal of Climate*, *16*, 2960–2978, 2003.

593 Taylor, K. E., R. J. Stouffer, and G. A. Meehl, An Overview of CMIP5 and the Experiment
594 Design, *Bulletin of the American Meteorological Society*, *93*, 485–498, 2012.

595 The GFDL Global Atmospheric Model Development Team, The New GFDL Global At-
596 mosphere and Land Model AM2-LM2: Evaluation with Prescribed SST Simulations,
597 *Journal of Climate*, *17*, 4641–4673, 2004.

598 Toggweiler, J. R., Climate change. Shifting westerlies, *Science (New York, N.Y.)*, *323*,
599 1434–5, 2009.

600 Toggweiler, J. R., and D. W. Lea, Temperature differences between the hemispheres and
601 ice age climate variability, *Paleoceanography*, *25*, PA2212, 2010.

602 Vallis, G. K., E. P. Gerber, P. J. Kushner, and B. A. Cash, A Mechanism and Simple
603 Dynamical Model of the North Atlantic Oscillation and Annular Modes, *Journal of the*
604 *Atmospheric Sciences*, *61*, 264–280, 2004.

605 Walker, C. C., and T. Schneider, Eddy Influences on Hadley Circulations: Simulations
606 with an Idealized GCM, *Journal of the Atmospheric Sciences*, *63*, 3333–3350, 2006.

Table 1. List of CMIP5 models used in the analysis. For all models, the first ensemble member ("r1i1p1") of the historical and RCP8.5 integrations was analyzed over the period 2000-2099.

	Model name	Institute
1	ACCESS1.0	CSIRO-BOM
2	ACCESS1.3	CSIRO-BOM
3	BCC-CSM1.1	BCC
4	BCC-CSM1.1(m)	BCC
5	BNU-ESM	GCESS
6	CanESM2	CCCMA
7	CCSM4	NCAR
8	CESM1-BGC	NSF-DOE-NCAR
9	CESM1-CAM5	NSF-DOE-NCAR
10	CMCC-CM	CMCC
11	CMCC-CMS	CMCC
12	CNRM-CM5	CNRM-CERFACS
13	CSIRO-Mk3.6.0	CSIRO-QCCCE
14	FGOALS-s2	LASG-IAP
15	FIO-ESM	FIO
16	GFDL-CM3	NOAA GFDL
17	GFDL-ESM2G	NOAA GFDL
18	GFDL-ESM2M	NOAA GFDL
19	GISS-E2-H	NASA GISS
20	GISS-E2-R	NASA GISS
21	HadGEM2-AO	MOHC
22	HadGEM2-CC	MOHC
23	HadGEM2-ES	MOHC
24	INMCM4	INM
25	IPSL-CM5A-LR	IPSL
26	IPSL-CM5B-LR	IPSL
27	IPSL-CM5A-MR	IPSL
28	MIROC-ESM	MIROC
29	MIROC-ESM-CHEM	MIROC
30	MIROC5	MIROC
31	MPI-ESM-LR	MPI-M
32	MPI-ESM-MR	MPI-M
33	MRI-CGCM3	MRI
34	NorESM1-M	NCC
35	NorESM1-ME	NCC

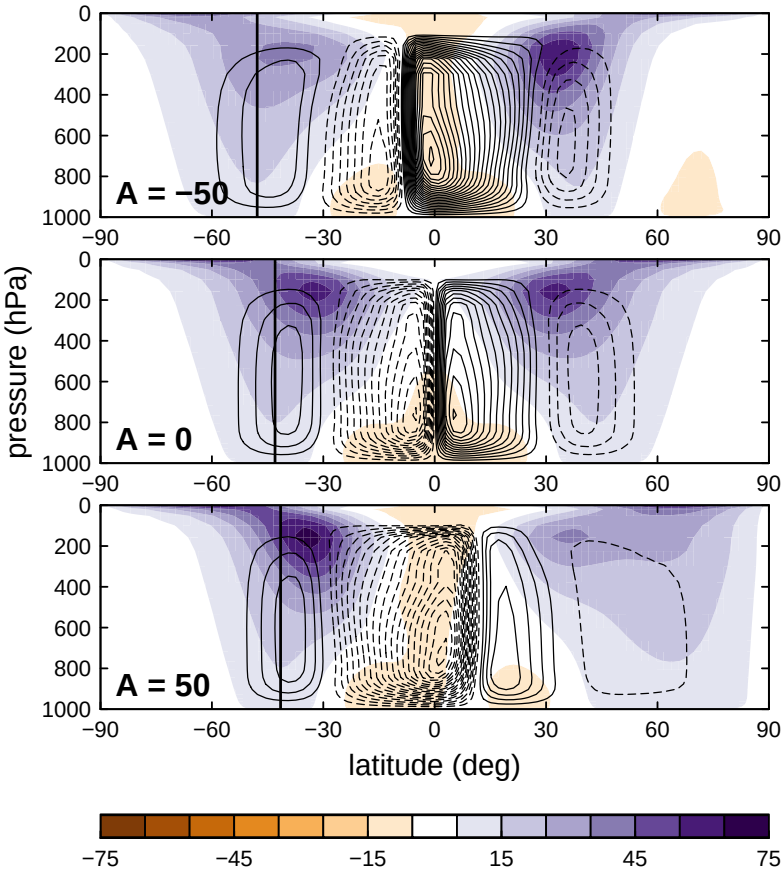

Figure 1. Climatological zonal-mean zonal wind (shading, in m s^{-1}) and mass streamfunction (contours, Sv) for three aquaplanet experiments with $A = (-50, 0, +50)$ W m^{-2} (see Eq. 1 and text for details). The zonal wind is shaded in intervals of 10 m s^{-1}, while the streamfunction is contoured every 20 Sv, with the zero contour omitted. The vertical line denotes the latitude of the eddy-driven jet.

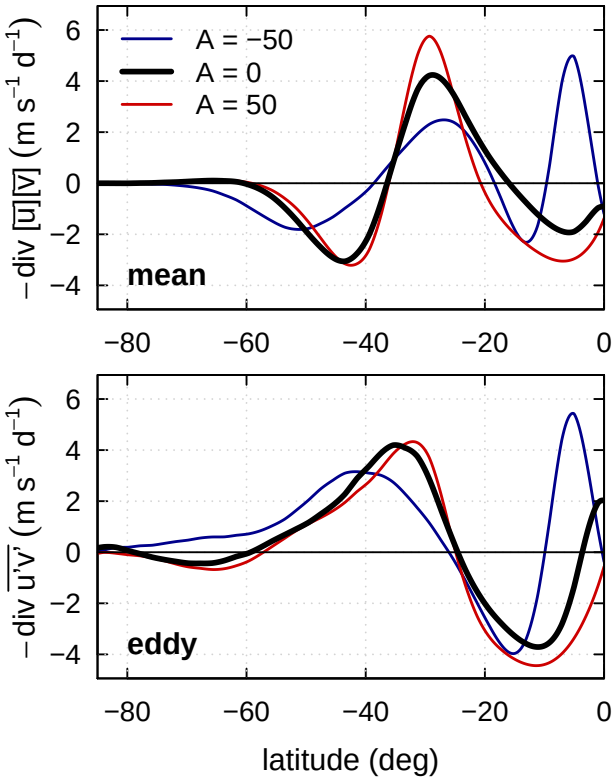

Figure 2. Upper-tropospheric momentum flux convergence in the SH by the mean circulation (top) and by eddies (bottom) in three aquaplanet experiments with $A = (-50, 0, +50)$ W m^{-2}. The values are vertically integrated between 150 and 300 hPa.

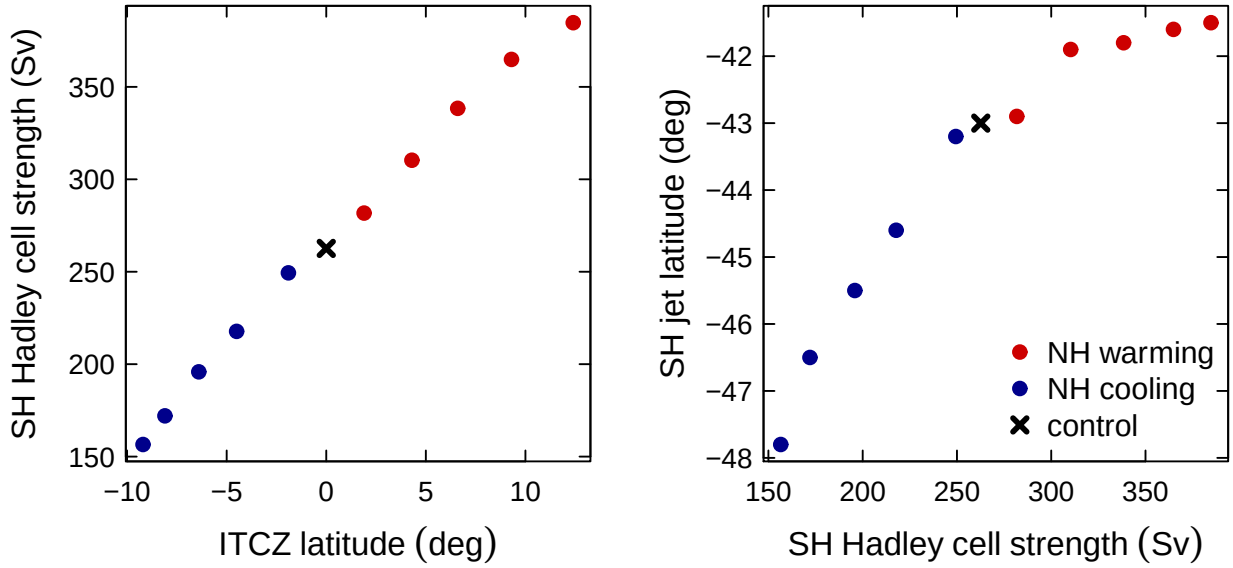

Figure 3. Left: strength of the SH Hadley cell as a function of the latitude of the ITCZ in the aquaplanet experiments. Right: SH eddy-driven jet latitude versus SH Hadley cell strength. The ITCZ is defined as the latitude where the streamfunction changes sign in the tropics at 500 hPa. The strength of the Hadley cell is expressed in Sverdrups (1 Sv = 10^9 kg s^{-1}).

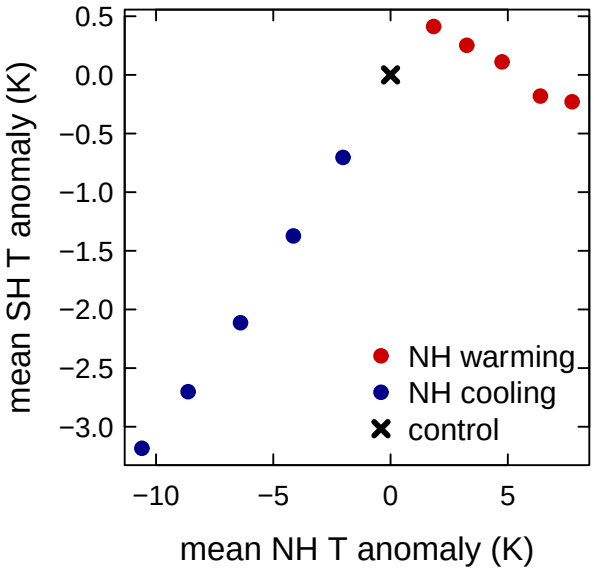

Figure 4. Hemispherically-averaged surface temperatures in the aquaplanet experiments.

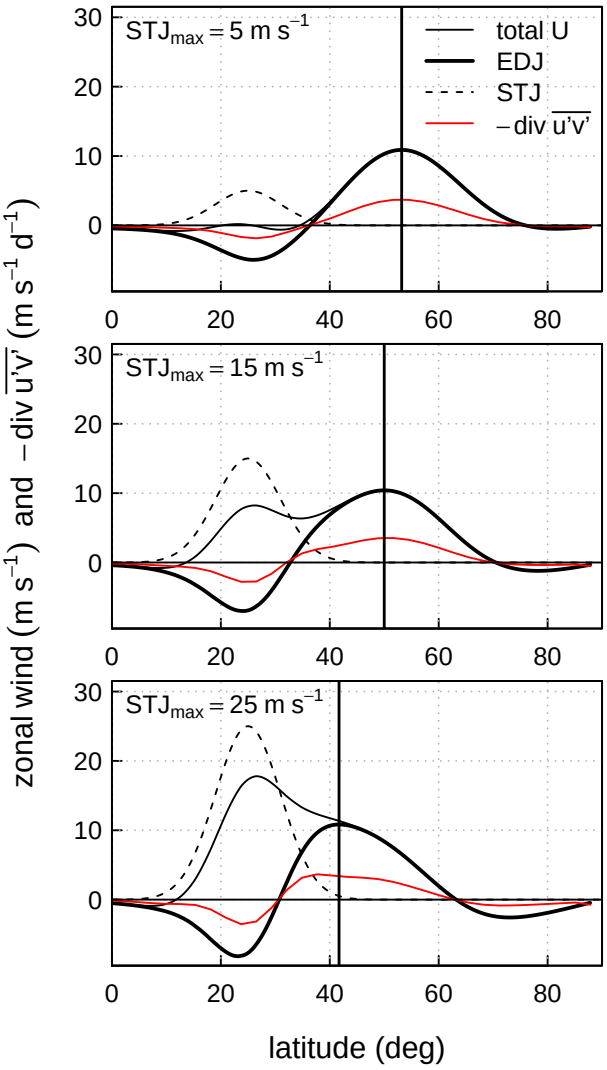

Figure 5. Zonal-mean zonal wind profiles and eddy momentum flux convergence in the barotropic model for different subtropical jet speeds. Shown are the total zonal wind (thin black), the eddy-driven component (thick), the prescribed subtropical jet (dashed), and the convergence of eddy momentum flux (thin red). Eddies are stirred at 50° latitude (see text). The vertical line denotes the mean eddy-driven jet latitude.

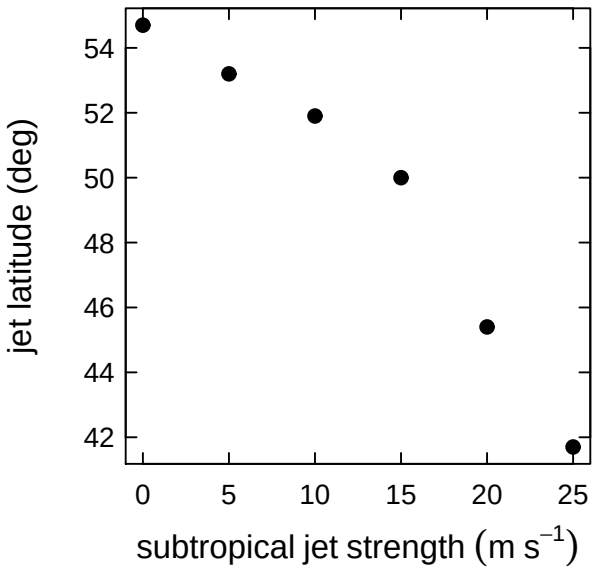

Figure 6. Latitude of the eddy-driven jet versus subtropical jet strength in the barotropic model experiments.

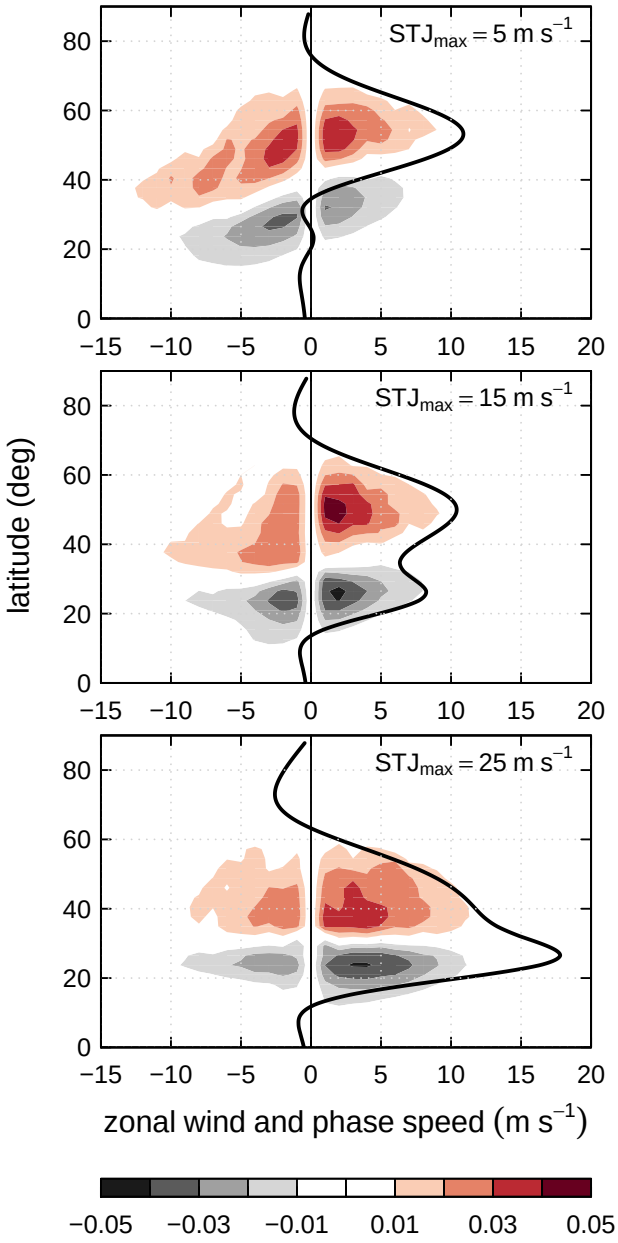

Figure 7. Latitude–phase speed power spectra of eddy momentum flux convergence (in m s^{-1} d^{-1}) times the cosine of latitude, $-\cos\phi \times \mathrm{div}\,\overline{u'v'}$, for the three barotropic model experiments presented in Fig. 5. The thick black curve denotes the total zonal wind.

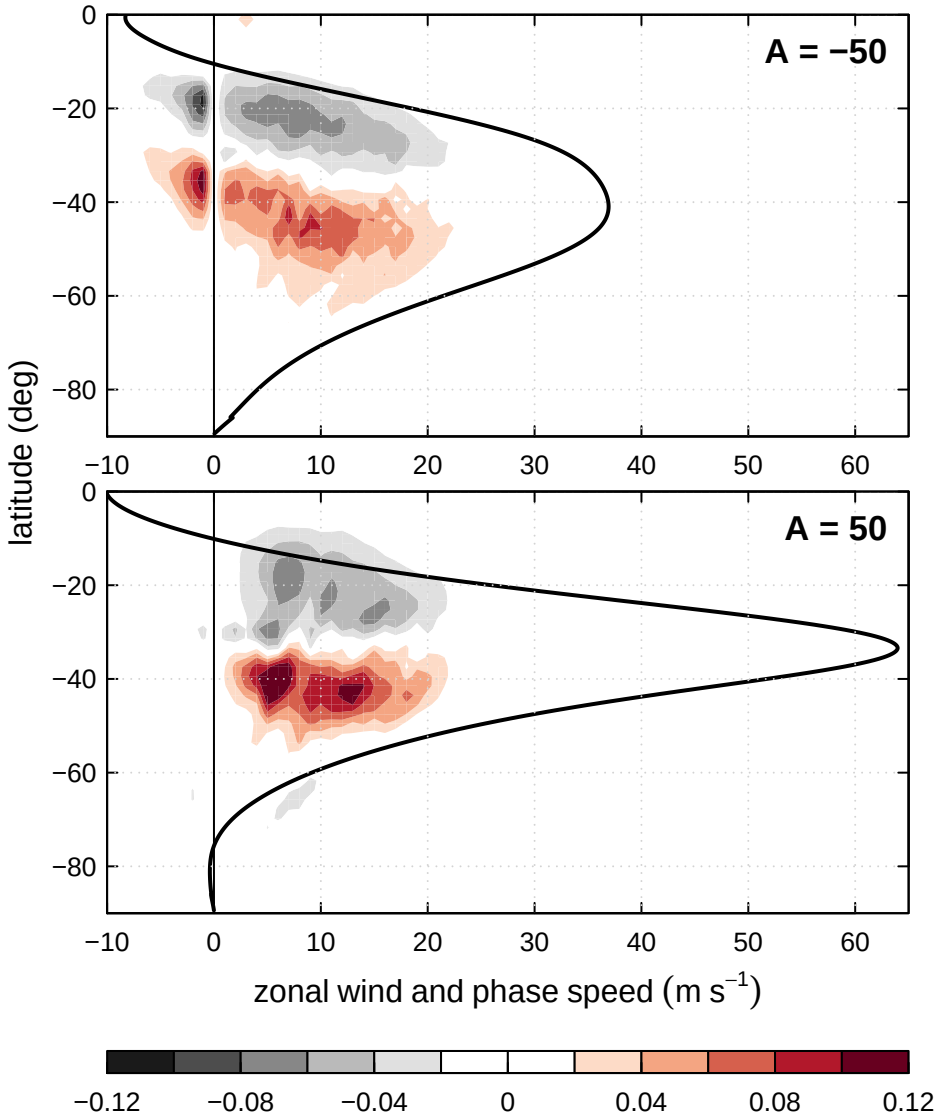

Figure 8. As in Fig. 7, but for the aquaplanet experiments with $A = \pm 50$ W m^{-2} at 225 hPa. The thick black curve denotes the zonal-mean zonal wind at that same level.

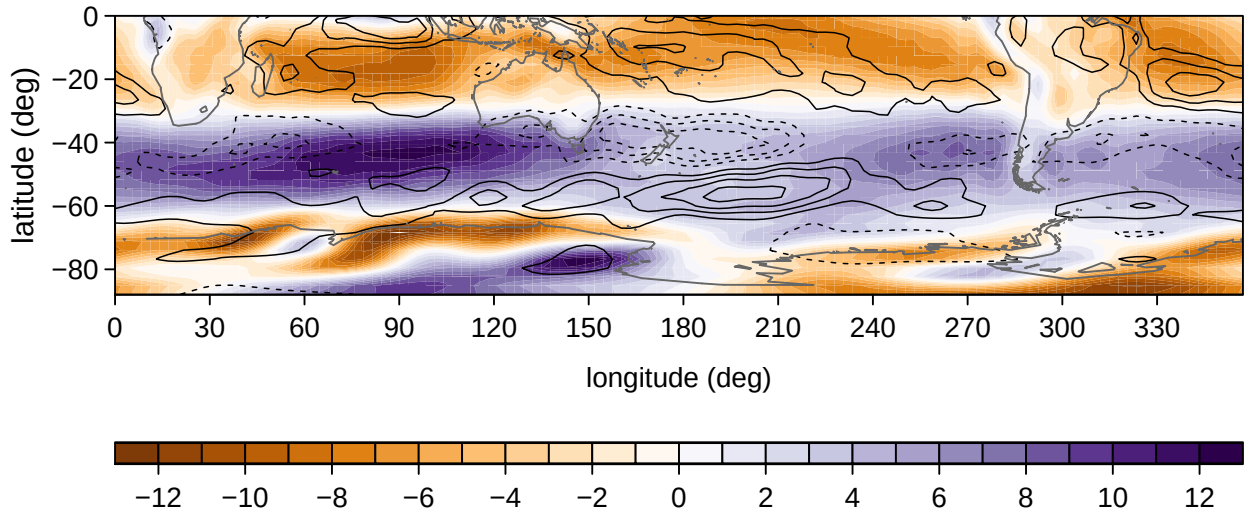

Figure 9. Austral winter (JJA) SH surface zonal wind in ECHAM model experiments. Shading denotes the mean zonal wind in m s^{-1}, while contours represent anomalies in the NH cooling experiment relative to the control. The contour interval is 0.5 m s^{-1}, with the zero line omitted.

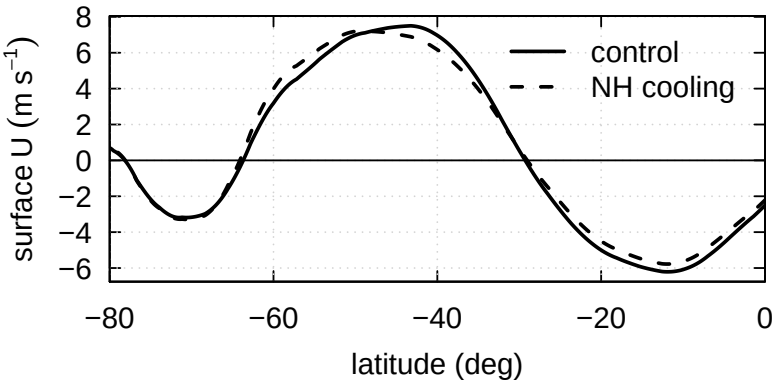

Figure 10. Zonally-averaged JJA surface zonal wind in ECHAM model experiments. Only the SH is shown.

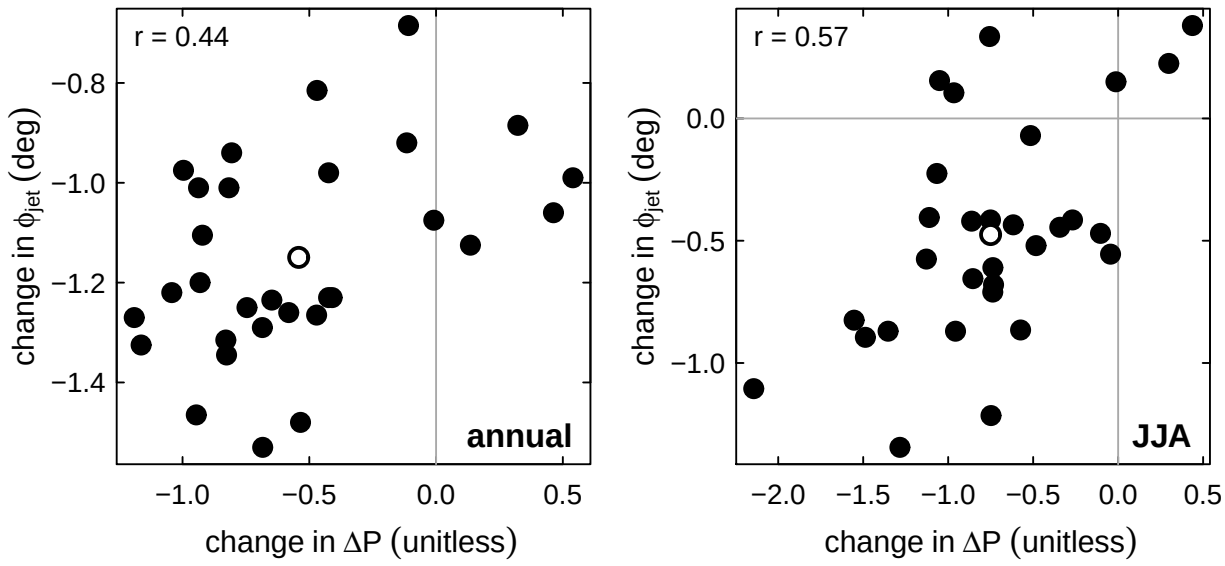

Figure 11. Change in SH jet latitude (ϕ_{jet}) versus change in tropical precipitation asymmetry (ΔP; see text) in integrations of a 30-member CCSM3 ensemble with prescribed A1B forcing. The change is computed as 2043–2062 minus 1980–1999 averages. Shown are annual-mean values (left) and JJA (right). Open circles denote the ensemble mean. Positive ΔP values correspond to an ITCZ in the NH.

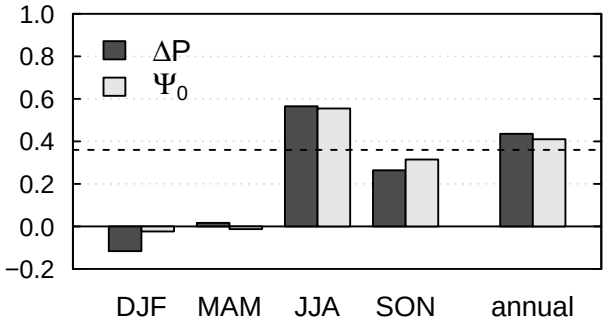

Figure 12. Correlation between change in jet latitude and in tropical circulation asymmetry among 30 CCSM3 ensemble members of a 21st-century climate simulation. The tropical circulation asymmetry is quantified by the tropical precipitation asymmetry ΔP and the cross-equatorial mass flux Ψ_0 (see text for details). The horizontal dashed line indicates the threshold for significance at the 5% level.

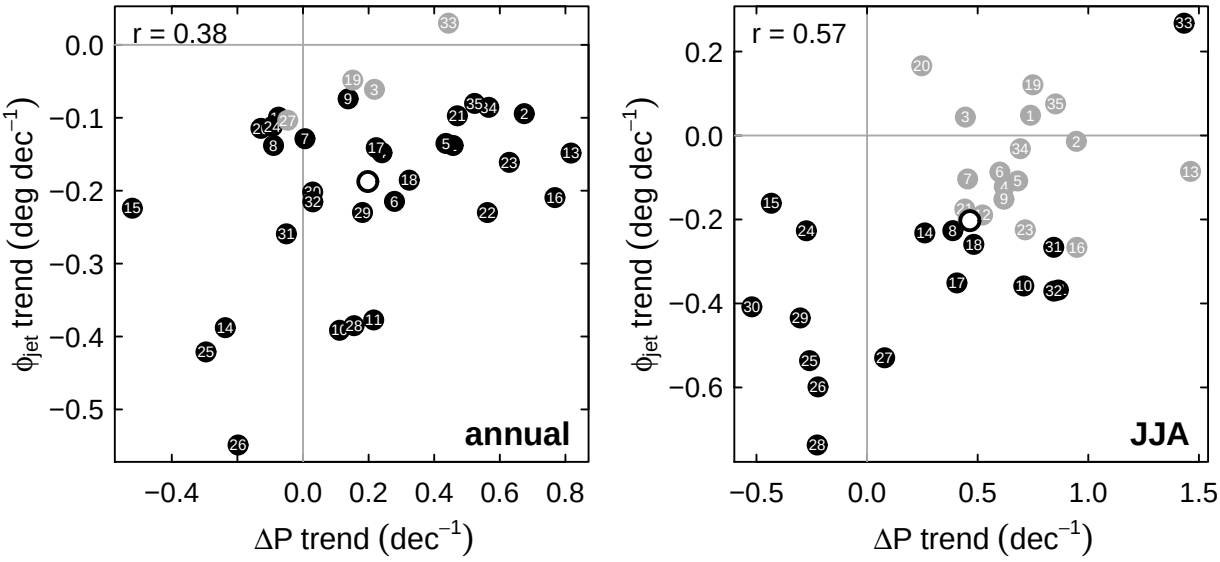

Figure 13. Trend in jet latitude ($\phi_{\rm jet}$) versus trend in ΔP in CMIP5 RCP8.5 integrations for the 21st century. Shown are annual-mean values (left) and JJA (right). The open circle denotes the multi-model mean, while gray dots indicate that the trend in $\phi_{\rm jet}$ is not statistically significant at the 5% level. The numbers refer to the models in Table 1. Negative trends in $\phi_{\rm jet}$ correspond to a poleward shift of the jet.

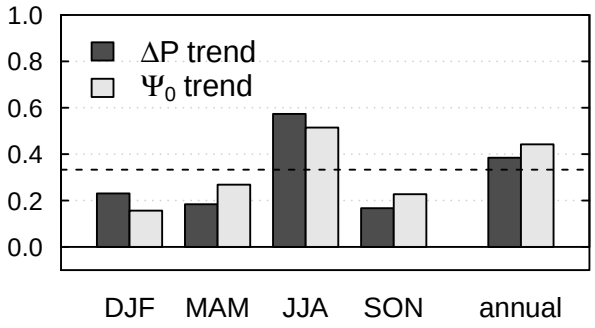

Figure 14. As in Fig. 12, but for trends in SH jet latitude and trends in tropical circulation asymmetry in CMIP5 RCP8.5 integrations. Both ΔP and Ψ_0 are defined such that positive trends correspond to a northward ITCZ shift.